

Integration of supercapacitors with enzymatic biobatteries toward more effective pulse-powered use in small-scale energy harvesting devices

Magdalena Skunik-Nuckowska · Katarzyna Grzejszczyk ·
Krzysztof Stolarczyk · Renata Bilewicz ·
Pawel J. Kulesza

Received: 31 July 2013 / Accepted: 11 December 2013 / Published online: 4 January 2014
© The Author(s) 2014. This article is published with open access at Springerlink.com

Abstract Effective integration of electrochemical devices consisting of enzyme-based biobatteries together with high power double-layer type capacitors is discussed here. An ultimate goal is to overcome a typical drawback of enzymatic power sources (biofuel cells and biobatteries): although their energy is potentially high enough to fulfill the needs of small electronic devices, their power is often too low. It is demonstrated that properly selected capacitor can support operation of such a low power device simply by supplying appropriate power pulses with fast dynamic response that is required for many applications involving fluctuating loads. Our model integrated system is obtained by coupling a series of double-layer capacitors with well-behaved zinc/oxygen biobattery. The biobattery utilizes a stable cathodic material composed of covalently phenylated single-walled carbon nanotubes and the oxygen reduction enzyme, laccase, together with the hopeite-covered zinc rod acting as the anode. The enzymatic power source was characterized by the maximum power density of 1.8 mW cm^{-2} , the open circuit voltage of 1.6 V. Nevertheless, under the 50Ω loading, the voltage of biobattery (electrode surface areas of ca. 0.3 cm^2) drops to 0 V after 2 s. The practical performance (power stability) of a biobattery has significantly improved by its parallel connection to electrochemical capacitor. The importance of such capacitor's parameters as low resistance (not more than a few hundred of milliohms), proper capacitance, and

leakage current (not higher than a few microamperes) is emphasized here. The potential utility of the optimized biobattery/supercapacitor system is discussed in terms of use as a source of power to operate a digital watch.

Keywords Integrated electrochemical system · Double-layer capacitor · Biobattery · Carbon nanotubes · Laccase-based cathode · Zinc anode · Enzymatic power devices

1 Introduction

During recent years, various enzymatic energy sources have attracted broad attention as cost effective and environmentally friendly alternatives for such energy conversion technologies as fuel cells and secondary batteries [1–7]. The energy produced during electrochemical processes occurring in the enzymatic cell (biofuel cell) is generally high enough to power small portable devices. Moreover, the presence of natural biological substances active in the pH close to neutral and operation in ambient temperatures allows for their direct implementation into the living organisms [3]. The energy produced in a typical biofuel cell originates from redox reactions involving the oxygen reduction (at cathode) and oxidation of such an organic fuel as glucose or ethanol (at anode). More recently, there has been growing interest in hybrid biofuel cells known as biobatteries that are expected to produce higher open circuit potentials and power densities in comparison to the conventional biofuel cells [8–11]. The whole concept of operation of so called non-rechargeable zinc–air batteries is based on simultaneous oxidation of zinc at the battery-type anode and the oxygen reduction at the enzymatic cathode.

There have been a number of enzymatic systems considered for construction of cathodes in both biofuel cells

M. Skunik-Nuckowska (✉) · K. Grzejszczyk · K. Stolarczyk ·
R. Bilewicz · P. J. Kulesza (✉)
Department of Chemistry, University of Warsaw, Pasteura 1,
02-093 Warsaw, Poland
e-mail: mskunik@chem.uw.edu.pl

P. J. Kulesza
e-mail: pkulesza@chem.uw.edu.pl

and biobatteries [12–14]. It is commonly accepted that the most promising results are obtained with use of multicopper oxidases, among which the simplest oxidase, laccase, has been probably the most intensively studied due to its ability to catalyze effectively the reduction of oxygen directly to water at relatively low overpotentials [8–11, 15–18]. Since proteins are macromolecules of largely developed and entangled structures, in which the catalytic centers are hidden inside the hydrophobic pocket, the distance between the enzyme's active center and the surface of electrode is usually too large for unimpeded direct transfers of electrons. To address this problem, various concepts for effective charge transfer mediation have been proposed [15, 19, 20]. It is noteworthy that, relative to many other enzymes, the laccase's active copper center is situated relatively close to the protein surface (ca. 0.7 nm); consequently, the development of mediator-free laccase-based materials capable of operating according to the direct electron transfer (DET) mechanism is feasible [21–24]. A promising approach has utilized single-walled carbon nanotubes (SWNTs) modified with anthraquinone and anthracene groups on the sides or at the ends of the nanotubes as novel materials permitting DET in the laccase containing catalytic films. Under such conditions, the 2D type electrode structure is transferred into the 3D assembly characterized by the effectively high enzyme population directly connected to the electrode thus leading to increase of the oxygen reduction currents. Such cathodes have been tested in hybrid biobatteries and produced the power density exceeding 2 mW cm^{-2} and the open circuit potential equal to 1.5 V [9].

Physicochemical stability of the biobatteries is generally sufficient enough to insure good operation under moderately high loads. Using a representative example [25], a biobattery maintained the voltage on a level of 0.6–0.8 V under 2.2 k Ω load for several days. But, many electronic devices (e.g., portable music players, watches, wireless communication systems, medical equipment), even if designed on small-scale, require power demands changing drastically with operating mode. Having in mind a rather small power density offered by enzymatic systems (at best on the level of few mW cm^{-2} [8, 9, 11]), it is reasonable to expect that a typical biobattery would not be able to deliver current pulses required for certain applications. Further, higher loads may lead to significant reduction of the biobattery lifetime or, even, to the performance failure and irreversible damage.

Electrochemical capacitors (supercapacitors) are often selected as power supports for various energy devices that include secondary batteries [26–30] and fuel cells [31–35], but, except a preliminary study [36], they have been barely so far considered as complementary power units coupled with enzymatic power sources. Electrochemical supercapacitors

offer important features including high specific power (up to 1 kW kg^{-1}), allowing for large amount of energy to be delivered in a short period of time at low cost per cycle and great durability [37–40]. Representative examples include simple systems starting from porous carbon-based double-layer capacitors [38, 41–44] to more complicated ones utilizing redox materials [45–48]. Having in mind high power applications, the capacitors involving only double-layer charging/discharging seem to be preferred due to their low internal resistance (on the level of milliohms), high output power, and fairly long lifetimes. When it comes to pulse power applications, the main drawback is in their high rate of self-discharge occurring as a side effect known as leakage current. This phenomenon, i.e., gradual loss of energy by a charged supercapacitor, will be considered here as the main limitation complicating application of supercapacitor as a device supporting operation of enzymatic power sources.

In the present work, we explore a biobattery utilizing the laccase-type-modified cathode, nanostructured with SWNTs terminally modified with phenyl groups, as active material toward oxygen reduction. A zinc rod covered with a protective film of $\text{Zn}_3(\text{PO}_4)_2$ (impermeable to oxygen) is used as the anode. The resulting biobattery is examined (alone or in parallel connection to a series of double-layer supercapacitors) under the high load regimes. Obviously the biobattery is a main source of energy, whereas the capacitor serves as an auxiliary one. Among the important supercapacitors' features is its ability to undergo fast charging/discharging so that high current may be delivered in a short time (milliseconds up to a few seconds). The supercapacitor would release its energy when the external device powered by a biobattery begins its operation, particularly when it requires a “peak current” to activate some of its functions or to change the operating mode (while a biobattery could be in a standby position). When it comes to potential applications (e.g., powering of the 1.5 V electronic watch), the choice of such capacitor's parameters as its capacitance, equivalent series resistance, and self-discharge rate should be carefully taken into consideration when a hybrid system is formed.

2 Experimental

2.1 Materials preparation

The *Cerrena unicolor* C-139 laccase samples lyophilized in vials were obtained from Prof. Rogalski (Department of Biochemistry, Maria Curie-Skłodowska University, Lublin, Poland), and they were isolated as described earlier [49]. The laccase stock solution activity determined after dissolving the protein powder (from vial) in 1 ml of MilliQ water was equal to 250 U mg^{-1} of protein.

The nanotubes modified with phenyl group on the end-walls (SWCNTs-PHEN-end) were obtained from Prof. Biernat and Dr. Zelechowska from Gdansk University of Technology, and they were synthesized as before [50].

2.2 Biobattery—assembly procedure

Biocathode The active layer was prepared on glassy carbon (GC) electrode (surface area, 0.07 or 0.28 cm²) which was initially polished using 0.05 μm alumina slurry (Buehler, USA) on polishing cloth. In the first step, the electrode was covered with ink-type suspension containing phenylated SWCNTs (4 mg of SCWNTs in 1 ml of 99.8 % ethanol) until the loading was equal to 570 μg cm⁻². The enzyme containing matrix was prepared by mixing the laccase solution (prepared by dissolving of 1 mg of enzyme in 1 ml of McIlvaine buffer/0.2 mol dm⁻³ NaNO₃, pH 5.2) and 1 % NafionTM solution (prepared by mixing of 5 % NafionTM solution from Sigma Aldrich with 99.8 % ethanol). The volume ratio was 1:1. Further, the 10 and 40 μl samples of thus obtained mixtures were dropped onto GC electrodes (of the areas, 0.07 and 0.28 cm², respectively); and they were allowed to dry under ambient conditions.

Bioanode The zinc rod (diameter 6 mm; from Merck, Germany) was at first dipped into 0.5 % of NafionTM in isopropanol (99.7 %) and let to dry. Thus, overcoated rod was further oxidized in the solution of 0.1 mol dm⁻³ phosphate buffer (pH 7) containing 0.15 mol dm⁻³ NaCl by application of a constant current of 13 mA cm⁻² for 15 h. This step led to the formation of stable and well-conductive hopeite layer (Zn₃(PO₄)₂) protecting the anodic material against corrosion in contact with the oxygen-saturated electrolyte [51]. The surface area of bioanode being in contact with the electrolyte was each time adjusted by wrapping the zinc rod with TeflonTM tape to obtain the same surface of both (biocathode and bioanode) electrodes, namely 0.07 or 0.28 cm².

2.3 Electrochemical characterization of capacitors

Two types of double-layer electrochemical capacitors were tested. They were commercially available activated carbon-based supercapacitors from Cellergy operating in aqueous electrolyte and characterized by the following parameters: capacitance $C = 25$ mF, operating charge/discharge voltage $U = 3.5$ V, equivalent series resistance $ESR = 300$ mΩ, and leakage current $i_{\text{leakage}} = 2$ μA, as well as Swagelok-type cells built of multi-walled carbon nanotubes (MWCNTs) pellets (1 cm in diameter) containing 90 wt% MWCNTs (Aldrich), 5 wt% acetylene black (Alfa Aesar), and 5 wt% PVDF (Aldrich) separated by glassy fibrous separator

(Aldrich) and immobilized between stainless steel current collectors. 1 mol dm⁻³ H₂SO₄ served as electrolyte. Two cells were further connected in series to increase the operating voltage. Finally, the following parameters were obtained: $C = 100$ mF, $U = 1.6$ V, $ESR = 800$ mΩ, and $i_{\text{leakage}} = 120$ μA. Additionally, in some of the tests, the commercial Cellergy capacitors were connected in parallel to increase the capacitance.

2.4 Instrumentation and electrochemical measurements

Electrochemical characterization was carried out using CH 660C Workstation (Austin, TX, USA) and digital multimeter with computer-based interface (Appa, Taiwan). All electrochemical measurements were done at 22 ± 2 °C. The current and power densities were expressed against geometrical area of the electrode.

Parameters of supercapacitors were evaluated from galvanostatic, amperometric, and impedance data. To determine the capacitance, the cells were galvanostatically charged to 1.6 V and then discharged to 0 V at constant current. The capacitance was calculated according to the formula: $C = It/U$, where I stands for the discharge current (A), t is the discharge time (s), and U is the discharge voltage (V). The equivalent series resistance was evaluated from the impedance Nyquist plots, namely from the intercept of the plot with the real axis, while the leakage current was obtained by charging the cells to 1.6 V for 2 h and, then, by measuring the current. Under the constant voltage conditions, the current flowing through the supercapacitor compensates the current leaking from the cell, and these parameters can be correlated with further self-discharge problems.

Electrocatalytic properties of the biocathode were investigated using the three-electrode arrangement utilizing Hg/Hg₂Cl₂ (KCl sat.) reference electrode, GC rod as the counter electrode, and GC disk (CHI, USA) as the working electrode (surface area of 0.07 cm²).

The biobattery parameters were determined in the oxygen-saturated 0.1 M McIlvaine buffer solution (pH 5.2) modified by the addition of 0.2 mol dm⁻³ of NaNO₃. The cell voltage was measured under the open circuit conditions, as well as under various loads ranging from 10 MΩ to 0.2 kΩ. The voltage was recorded after 5 s following application of each load.

To comment on influence of the presence of supercapacitor on the power output of the biobattery, the zinc-oxygen power source alone, or in parallel connection with supercapacitor (or series of supercapacitors), was subjected to a continuous pulse work under the 200 or 50 Ω load (depending on the biobattery's electrode surfaces). The pulse time was 2 s.

3 Results and discussion

3.1 Electrocatalytic properties of SWCNTs-PHEN-end/laccase system toward O_2 reduction

In order to investigate the electrocatalytic activity of the cathodic material (used for the construction of the biobattery), a series of voltammetric experiments were conducted. Figure 1 illustrates responses of GC electrode modified with terminally phenylated SWNTs covered with a matrix containing laccase dispersed in NafionTM solution. The final concentration of NafionTM in the mixture was 0.5 %. The responses were recorded in the absence, i.e., in the nitrogen-saturated solution (Fig. 1a), and in the presence of oxygen (Fig. 1b). The onset potential (determined at 1 mV s^{-1}) for the electrocatalytic process was equal to 0.58 V (vs. $\text{Hg}/\text{Hg}_2\text{Cl}_2$), and the current density (measured at 0.15 V) was equal to $395 \mu\text{A cm}^{-2}$. The latter value was approximately twice higher than that reported earlier for the system utilizing SWNTs phenylated on the side walls [9]. The results were highly reproducible (within 5 %) during at least ten independent experiments.

3.2 Electrochemical characterization of biobattery

The electrode was further tested within the hybrid biobattery equipped with hopeite-covered Zn rod acting as an anode. The power density–voltage and the current density–voltage dependencies were plotted against external loads applied between the anode and the cathode (from $10 \text{ M}\Omega$ to $0.2 \text{ k}\Omega$). To minimize the power losses due to the oxygen depletion during the tests, the resistance pulses were each time limited

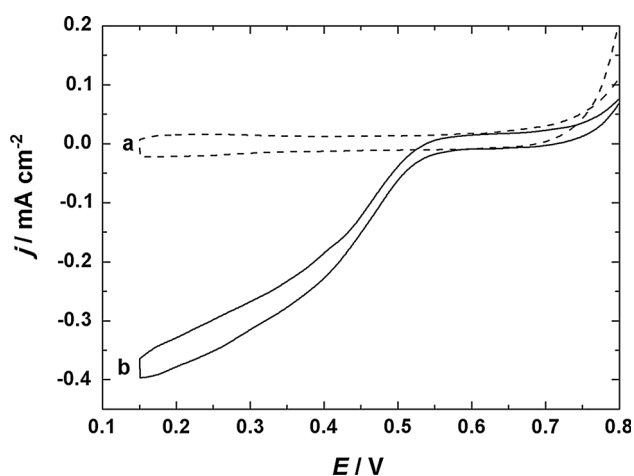


Fig. 1 Cyclic voltammetric response of GC electrode modified with phenylated SWCNTs (SWNTs-PHEN-end) and covered with NafionTM/laccase matrix recorded in (a) deoxygenated, (b) saturated with oxygen McIlvaine buffer/ $0.2 \text{ mol dm}^{-3} \text{ NaNO}_3$ (pH 5.2). Scan rate: 1 mV s^{-1} . Electrode surface: 0.28 cm^2

to 5 s. The results are presented in Fig. 2a. The open circuit voltage measured for the system before the load application was equal to 1.65 V. The maximum power density of ca. 0.5 mW (1.8 mW cm^{-2}) was achieved under the load of $1 \text{ k}\Omega$ at the voltage of 0.7 V (Fig. 2b). Such low level of power density is a serious limiting factor when it comes to applications of the enzymatic energy sources requiring high current bursts. As it is apparent from Fig. 2a (green plot), the higher the output current, the lower voltage output was produced by the biobattery. For example, the current of 1.1 mA (ca. 4 mA cm^{-2}) drained from the system causes a drastic voltage drop from 1.65 V down to 0.2 V thus precluding practical application of the biobattery. To keep biobattery at the maximum power output conditions (Fig. 2a, blue plot), the output current cannot exceed 0.7 mA (2.5 mA cm^{-2}). The discussed parameters significantly change when the system operates for longer periods of time. The likely features such as oxygen depletion

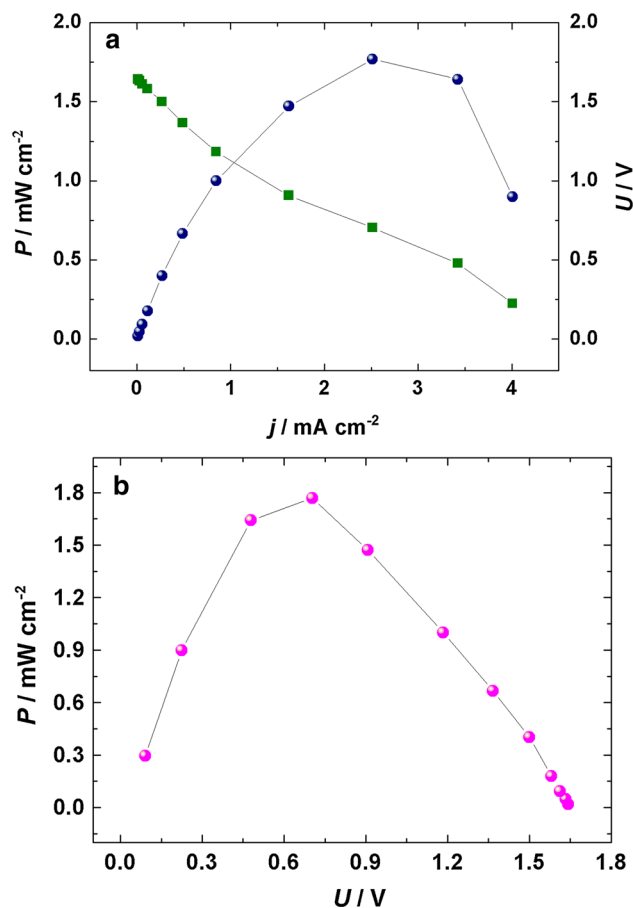


Fig. 2 Dependence of power density (blue coloured filled circle) and cell voltage (filled square) on current density (a) and power density (pink coloured filled circle) on cell voltage (b) plotted for laccase-based zinc–oxygen biobattery built of $\text{Zn}/\text{Zn}_3(\text{PO}_4)_2$ anode and SWCNTs-PHEN-end/laccase/NafionTM cathode. Electrolyte: oxygen-saturated McIlvaine buffer/ $0.2 \text{ mol dm}^{-3} \text{ NaNO}_3$ (pH 5.2). Electrode surfaces: $A = 0.28 \text{ cm}^2$

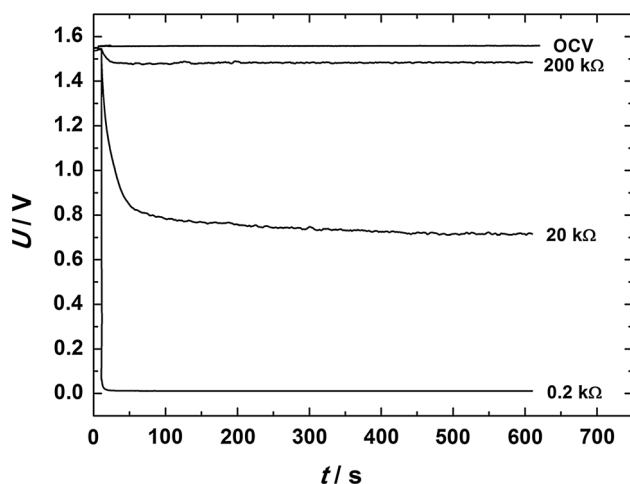


Fig. 3 Voltage–time dependence recorded for laccase-based zinc–oxygen biobattery operating in open circuit voltage conditions (OCV) as well as during application (600 s) of resistances: 0.2, 2, and 20 k Ω . Electrode surfaces: $A = 0.07 \text{ cm}^2$, $P_{\text{max}} = 0.13 \text{ mW}$. Electrolyte: oxygen-saturated McIlvaine buffer/ $0.2 \text{ mol dm}^{-3} \text{ NaNO}_3$ (pH 5.2)

occurring near the electrode surface or kinetic limitations in the cathodic reaction would lead to the further drop of voltage as demonstrated in Fig. 3. For all external loads applied, the steady-state voltage is readily reached, and this behavior refers to the real behavior of biobattery under standby conditions. Using the data of Fig. 3, the steady-state current recorded after 600 s of the biobattery's operation has been found to be equal to: 0.1 mA cm^{-2} at 20 k Ω , 0.5 mA cm^{-2} at 2 k Ω , and 0.7 mA cm^{-2} at 0.2 k Ω . Obviously the current recorded upon application of the lowest resistance is the highest, nevertheless, the corresponding voltage tends to drop to 0 V thus making the biobattery useless while operating under conditions of such loads.

To elucidate the biobattery behavior under conditions demanding peak currents, the device was subjected to a series of short (2 s each) loads (200 Ω “pulses”) for 7 h. The results are shown in Fig. 4. It can be observed that, at the beginning of diagnostic tests, the open circuit voltage was equal to 1.63 V, but it immediately dropped down to almost 0 V after each pulse. Thus, in practice, virtually any device powered by the biobattery would be practically switched off. Obviously, the current could be continuously produced by the cell as a result of electrochemical reactions, and the voltage recovery would be expected in ca. 20 min. We noticed that the continuous pulse operation led to a slow and gradual decrease in the initial value of voltage available under open circuit conditions, most probably due to the irreversible degradation of the enzyme structure caused by application of high external loads.

The above results are consistent with the view that biobatteries are not suitable devices for operation when high power pulses are required. This problem can be solved

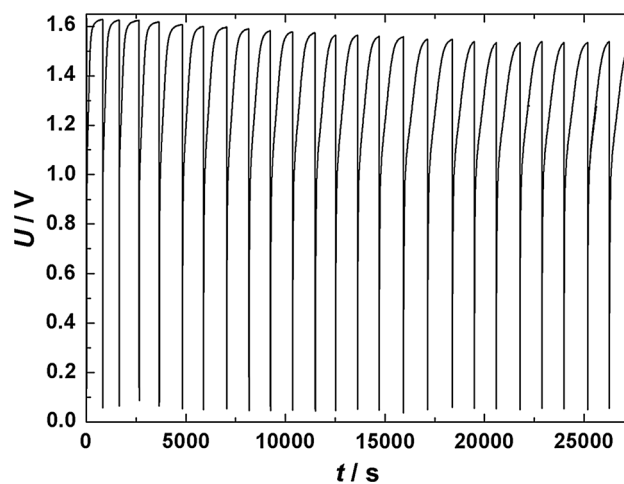


Fig. 4 Variation of laccase-based zinc–oxygen biobattery voltage versus time upon application of external loads of 200 Ω for 2 s. Electrode surfaces: $A = 0.07 \text{ cm}^2$, $P_{\text{max}} = 0.13 \text{ mW}$. Electrolyte: oxygen-saturated McIlvaine buffer/ $0.2 \text{ mol dm}^{-3} \text{ NaNO}_3$ (pH 5.2)

in two ways: either (i) by the increase of the electrodes surface area or (ii) by combining biobattery with external high power device. The first solution is rather difficult to realize, because modern electronic devices are intended to be miniaturized. With respect to the second solution, we refer here to the earlier study [36] describing the data concerning integration of enzymatic biobattery with two electrochemical capacitors connected in series. The resulting hybrid system was subjected every 20 min to high current pulses of 5 mA each lasting for 3 s. Integration with high power supercapacitors led to stabilization of the voltage output of biobattery on the constant level of ca. 1.1 V for 35 h. Obviously, the choice of such supercapacitor's parameters as resistance, capacitance, and leakage current is crucial to successful operation of the hybrid system. Our observations and recommendations are discussed in the next section.

3.3 Enhancement of biobattery's power level through combination with supercapacitor

Figure 5 illustrates a hybrid system obtained by integrating the zinc–oxygen biobattery with the carbon/carbon double-layer type electrochemical capacitor. The capacitor was placed in parallel to the biobattery, and it was connected to the resistance decade simulating various external loads. To monitor and control passing current and generated voltage, potentiostat and multimeter were also included in the network. The switch between the biobattery and supercapacitor allows for quick connection/disconnection of supercapacitor.

High internal resistance is one of the key factors responsible for the low power output of enzymatic

biobattery. The resistive limitations may originate from the ohmic resistance of electrolyte or electrode materials, the mass transport resistance, and, predominantly, from the charge transfer resistance assigned to the slow kinetics of bioelectrochemical reactions [52]. Thus, there is need for a low internal resistance supercapacitor to be used as an auxiliary device supporting possible higher power applications. Generally, the lower the capacitor's resistance, the lesser the restrictions in its ability to act as an effective supporting device. The carbon/carbon supercapacitors utilized by us were characterized by acceptable resistances on the level of milliohms. In particular, the resistances were on the level of ca. to 300 m Ω for a single commercial cell and 400 m Ω for single Swagelok-type cell utilizing MWCNTs. At the operating voltage of 1.6 V, the maximum power of the supercapacitor was calculated according to the formula:

$$P_{\max} = \frac{U^2}{4ESR} \quad (1)$$

where P_{\max} is the maximum power, and other parameters have been described earlier. The maximum power values determined for the investigated cells were in the range from 0.8 to 2.1 W depending on the cell type and assembly (i.e., connection in parallel or in series). Obviously, the resistance was doubled when two supercapacitors were connected in series aiming at increasing the system's overall voltage output (e.g., the case of Swagelok-type cells

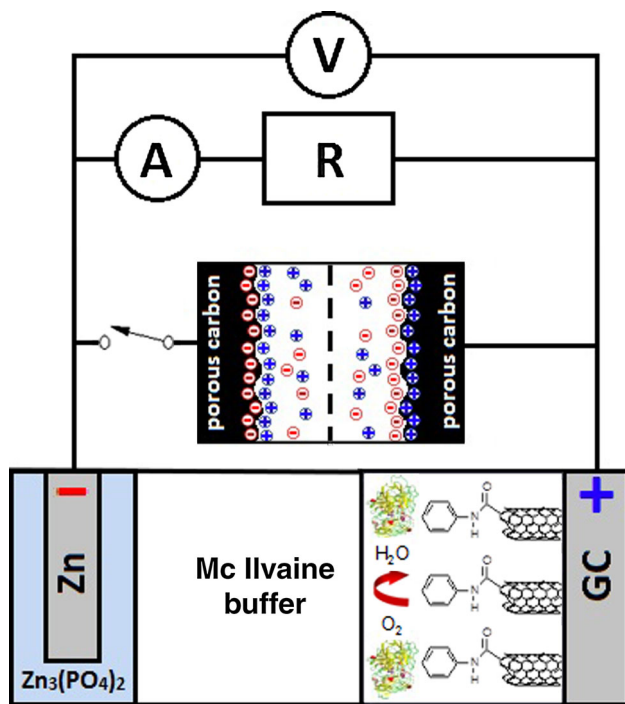


Fig. 5 Schematic representation showing the connection and operation rules of integrated laccase-based zinc–oxygen biobattery and supercapacitor

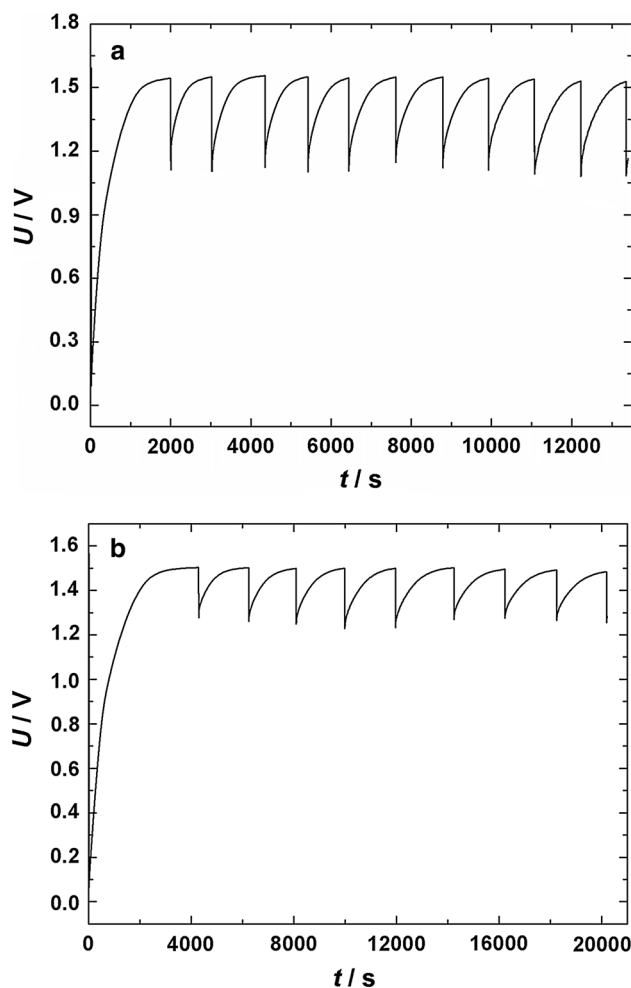


Fig. 6 Voltage changes across 0.13 mW laccase-based zinc/oxygen biobattery (electrode surfaces: $A = 0.07 \text{ cm}^2$), connected in parallel to: **a** 25 mF, **b** 50 mF supercapacitor recorded during application of external load of 200 Ω for 2 s

utilizing carbon nanotubes). Due to the relatively lower resistivity, double-layer type capacitors are preferred over redox-type capacitors for integration with such a low power device as biobattery.

As already mentioned, when the voltage drop across the biobattery (upon application of high external load) is too large, the device will not work properly. Figure 6 illustrates how the presence of supercapacitor influences the voltage–time characteristics. In the present study, the biobattery (with electrode surface areas of 0.07 cm^2) was characterized by power of 0.13 mW, and it was coupled with commercial carbon/carbon supercapacitors characterized by variable capacitances. Figures 6a and b show the potential (U)–time (t) responses obtained for the 0.13 mW laccase-based zinc/oxygen biobattery connected in parallel with the 25 and 50 mF supercapacitors (they were discharged to 0 V before connection to the circuit). The capacitance of 50 mF was achieved by connecting two

25 mF single cells in parallel. At the beginning, i.e., under open circuit conditions, the biobattery produced the maximum voltage of ca. 1.6 V. Once the circuit was closed, the biobattery started to deliver current to the discharged supercapacitor. The charging time was obviously dependent on the capacitance values, and within ca. 35 and 70 min, the maximum voltages of 1.54 and 1.5 V were obtained for the biobattery systems connected with the 25 and 50 mF supercapacitors (Fig. 6a, b), respectively.

In the next step, the external loads of 200 Ω were applied for 2 s to the systems. For comparison, the 0.13 mW biobattery operating as a single device (Fig. 4) and subjected to such an extreme load responded with a rapid decrease of voltage from 1.6 V to almost 0 V. In the presence of supercapacitors, the voltages were maintained on the levels of 1.1 V (Fig 6a) and 1.3 V (Fig. 6b). The differences in the observed voltage drops should be attributed to the different amounts of energy supplied by supercapacitors characterized by different capacitances. The amount of energy utilized depends on the power demand and the time for which the system is used according to the equation:

$$P_{\text{load}} = \frac{E_{\text{cap}}}{t} \tag{2}$$

where E_{cap} is the energy provided by electrochemical capacitor, P_{load} is the required power, and t is the time during which the energy is delivered.

Having in mind the fact that supercapacitor’s energy is directly proportional to its capacitance, it is reasonable to expect that during the same period of time (2 s), the 50 mF supercapacitor would be able to deliver more power than the cell of smaller capacitance (25 mF). Consequently, the utilization of 50 mF capacitor should lead to a smaller voltage drop (Fig. 5b). Therefore, the capacitance should be adjusted to assure an energy balance that can be understood as follows:

$$E_{\text{cap}} = E_{\text{load}} \tag{3}$$

$$\frac{1}{2} C_{\text{cap}} (U_0^2 - U_1^2) = P_{\text{load}} \times t \tag{4}$$

where C_{cap} is the required capacitance, U_0 is the initial supercapacitor voltage, U_1 is the minimum voltage to which a supercapacitor can be discharged at the end of the peak load, and E_{load} stands for the load energy that can be calculated as the required power (P_{load}) multiplied by load duration (t).

Having in mind the above considerations, the capacitance can be easily found as:

$$C_{\text{cap}} = 2 \frac{P_{\text{load}} \times t}{U_0^2 - U_1^2} \tag{5}$$

It is important to note that the Eq. 5 does not include the supercapacitor’s resistance (ESR). Nevertheless, having in

mind that supercapacitors are generally characterized by low equivalent series resistance, i.e., it can be assumed that $ESR \ll U_1$, and, therefore, it can be typically neglected.

For more detailed characterization, the data of Figs. 4 and 6b have been considered to comment on the energy and power capabilities during the system’s operation for 2 s under the load of 200 Ω. Consequently, the biobattery/supercapacitor hybrid system is characterized (vs. simple biobattery) by the following parameters: power, 8.5 mW (vs. 0.013 mW); energy, 17 mJ (vs. 0.025 mJ); and power capacity, 4.7 μWh (vs. 0.007 μWh).

Considering the applications of supercapacitor as an auxiliary device for bioelectrochemical power sources and realizing that its task is to recharge the supercapacitor between the power pulses, the charging mechanism has been carefully investigated by us. When the circuit of Fig. 5 has been closed, the biobattery has started to deliver the current to discharging supercapacitor. Simultaneously, the current flowing through the circuit and the voltage produced were recorded. The results are presented in Fig. 7. The inset to Fig. 7 illustrates the charging characteristics (voltage–time dependence) for the 25 mF supercapacitor connected in parallel to 0.13 mW laccase-based zinc–oxygen biobattery. The plot is nonlinear, and it is characteristic of the case involving charging at constant current. In other words, the current injected into the cell changes with time, and, therefore, the exponential-type response appears. This situation has been confirmed in the course of direct current measurements (Fig. 7a). As it can be seen, the current which is transferred from the biobattery reaches 0.1 mA at the beginning of charging (short circuit of the cells) and tends to decay rapidly with time. After ca. 2,000 s, the biobattery delivers only 13 μA

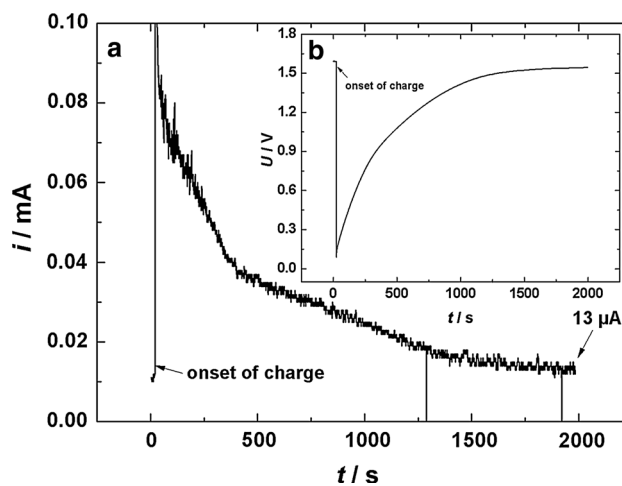


Fig. 7 Charging of 25 mF supercapacitor by laccase-based zinc/oxygen biobattery (0.13 mW) (electrode surfaces: $A = 0.07 \text{ cm}^2$). **a** monitoring of current flowing from biobattery to supercapacitor and **b** voltage changes in the circuit

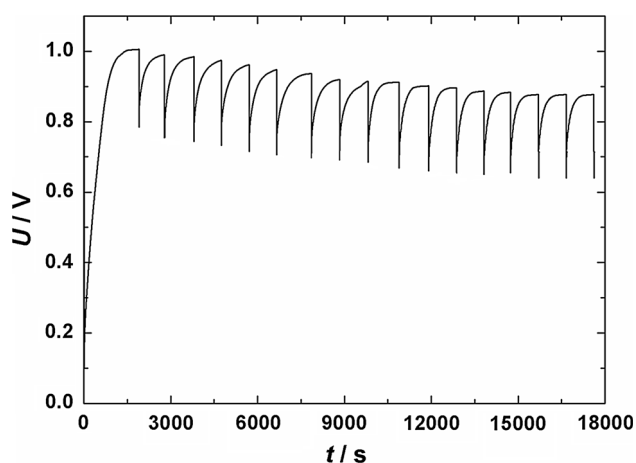


Fig. 8 Voltage changes across 0.5 mW laccase-based zinc/oxygen biobattery (electrode surfaces: $A = 0.28 \text{ cm}^2$) connected in parallel to 100 mF Swagelok-type supercapacitor (two cells in series) recorded during application of external loads of 50Ω for 2 s. Supercapacitor material: 90 wt% MWCNTs, 5 wt% acetylene black, and 5 wt% PVDF. Supercapacitor electrolyte: $1 \text{ mol dm}^{-3} \text{ H}_2\text{SO}_4$

resulting in the saturation of the supercapacitor and in appearance of the almost steady-state voltage in the system (Fig. 7b). In the configuration considered by us, the final voltage is very close to the open circuit voltage of the biobattery itself, and it is equal to 1.55 V. It should be attributed to the following features: (i) sufficiently low capacitance (25 mF), and (ii) almost negligible leakage current ($2 \mu\text{A}$). Our further deliberations will concentrate on the influence of these two factors on the performance of the biobattery/supercapacitor hybrid system.

Figure 8 refers to the operation of the 0.5 mW biobattery (electrode areas, 0.28 cm^2) under the load of 50Ω but following connection to two Swagelok-type cells [38] utilizing multi-walled carbon nanotubes as electrode materials and operating in 1 mol dm^{-3} sulfuric acid. The main goal of this study has been to show how the leakage current occurring in the cell affects performance of the integrated system. The self-discharge process induced by the leakage current is defined as a spontaneous and gradual voltage loss observed in the charged supercapacitor. The higher the leakage current, the faster the voltage decay will occur, thus resulting in overall power decrease. Generally, the leakage current can be produced as the effect of following processes: (i) electrochemical decomposition of the electrolyte (when the charging/discharging takes place beyond the thermodynamic potential window of the electrolyte), (ii) parasitic reactions related to the material's and electrolyte's impurities, (iii) presence of oxygen in the electrolyte and its reduction at the negative electrode, (iv) non-uniform distribution of charge within the deep pores of electrode material dependent on the pore structure and its geometry (regarded to be a predominant effect), and (v) the presence of short-circuits as a result of not

sufficient isolation of electrodes [53]. When the supercapacitor is used together with enzymatic power source, the leakage current should be as low as possible. These requirements are much more severe than for other integrated systems including batteries or fuel cells and supercapacitors. To achieve an acceptable level of few μA (as in commercial supercapacitors used in our previous investigations), it is necessary to optimize the manufacturing procedures to insure the quality control and eliminate the parasitic factors. The carbon nanotubes-based supercapacitor used in our studies (Fig. 8) was characterized by the leakage current of $120 \mu\text{A}$. Having in mind a very low output current supplied by the biobattery which exponentially decreases when the voltage across supercapacitor grows (Fig. 7), it is reasonable to expect that the rate of supercapacitor's leakage will be faster than the rate of charging. This phenomenon would result in incomplete charging which stops when the current produced by the biobattery reaches the value of the leakage current. For this reason, the maximum voltage obtained for the investigated system was equal to 1 V at the beginning of operation and had a tendency to decrease in time which can be attributed to the leakage current fluctuation or/and the biobattery aging. The problem with complete charging might also occur when the charge storage device used is characterized by too high capacitance. Assuming that the leakage current is on the level of few μA , theoretically, the charging process should proceed without any difficulties. However, a very small amount of charge injected to the supercapacitor, additionally decreasing with time, could make the process extremely (unrealistically) time consuming.

To comment the potential utility of the proposed hybrid configuration, a 1.5 V electronic watch has been chosen as the device to be powered by 0.5 mW laccase-based zinc/oxygen biobattery (electrode surface area, 0.28 cm^2) connected in parallel to the 50 mF (obtained by connection of two commercial carbon/carbon cells in parallel) low leakage current ($4 \mu\text{A}$) supercapacitor in the circuit equipped with the switch allowing for quick connection and disconnection of supercapacitor. The power provided by a biobattery is high enough to operate the watch under standby or passive conditions, i.e., without using of any of its special functions. When the input current is equal to ca. $10 \mu\text{A}$, only a slight voltage drop across the biobattery, namely from 1.6 V (labeled as 1 in Fig. 9a) to 1.57 V (labeled as 2 in Fig. 9a) has been observed. The stability test (Fig. 9b) shows that that the biobattery's operating voltage under standby conditions can be held at a constant level for 10 h while the measurements performed in air-saturated solution (not shown here) confirmed the good stability (voltage decay on the level of 5 %) during several days. However, when the watch is used in the different operating modes (light up, alarm) requiring higher input currents, the powered device has immediately switched off, because the biobattery was

not able to maintain the required voltage (1.05–1.5 V). For example, the voltage drop occurring in the circuit following activation of the light up function for 2 s (marked as 3) is illustrated in Fig. 9a (navy-blue line). The system's voltage has immediately decreased to 0.6 V, and it has occurred to be too low for further operation of the watch until the biobattery is recovered to at least 1.05 V. In contrast, when the 50 mF supercapacitor has been introduced to the circuit, the voltage drop following switching on the light up function is significantly lower [namely, it decreased to only 1.4 V during 2 s (Fig. 9a, pink line)]. When the light up function has been switched off, the biobattery has started to operate in the standby mode again (labeled as 4 in Fig 9a) permitting simultaneous recharging of the supercapacitor. Following 1,000 s of testing, the charged supercapacitor can be disconnected leaving the biobattery as the main power source for the watch. Although the positive effect of a supercapacitor on the power capability of a biobattery is unquestionable, it is noteworthy that the capacitor's presence somewhat limits supply of energy from the biobattery. This "overhead of hybridization" refers to the system's energy loss originating from the supercapacitor's leakage current that must be continuously compensated by the biobattery. Namely, 4 μA is taken out from the biobattery during recharging of the supercapacitor as well as during holding its voltage at constant value while operating under standby condition. By taking into account proportionality of the leakage current to the terminal voltage of supercapacitor, the energy loss has obviously found to be lower at the lower voltage, but it is still on the level of 0.5–0.6 mJ. To summarize, we demonstrate that coupling of the auxiliary storage device (supercapacitor) together with the enzymatic power source (biobattery) is of primary importance to its stable operation under conditions of the fluctuating loads (that would otherwise reduce the biobattery's performance during longer periods of time). Future research would require better control and minimizing of the current loss parameters of supercapacitors. These features are crucial to further development of bioelectrochemical energy sources that could operate in practice without energy losses and power deficiencies.

4 Conclusions

We demonstrate here that the combination of electrochemical capacitor together with biobattery can significantly improve the power performance of the enzymatic biobattery (that otherwise low power device) and, consequently, prolongs its practical life-time. As model enzymatic system, the well-behaved mediator-free zinc/oxygen biobattery utilizing a GC electrode decorated with phenylated SWNTs/laccase and

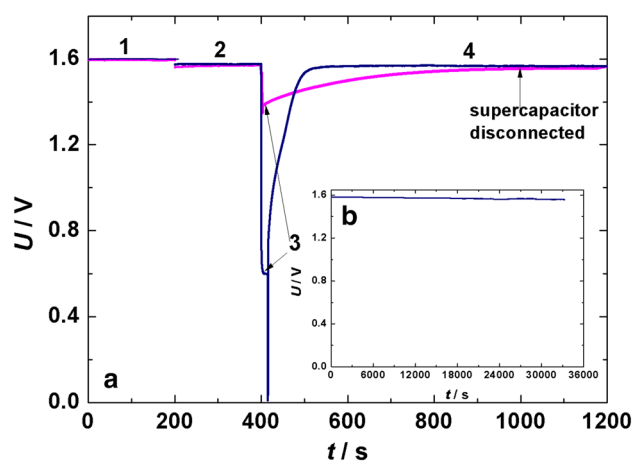


Fig. 9 a Voltage changes across 0.5 mW laccase-based zinc/oxygen biobattery used to run a digital watch recorded in standby conditions (labeled as 2 and 4) and during high input current mode (3) in the absence (navy-blue plot) and in the presence (pink plot) of 50 mF supercapacitor in the circuit. Inset b represents the voltage versus time dependence in standby conditions

$\text{Zn}_3(\text{PO}_4)_2$ -covered zinc rod has been used. The biobattery itself has been characterized by high open circuit voltage exceeding 1.6 V and a power density of ca. 1.8 mW cm^{-2} . Although the power density has been found to be among the highest reported so far, its level is still insufficient for applications requiring high external loads: under such condition, the biobattery's voltage tends to rapidly drop to 0 V. A conventional parallel connection with carbon/carbon double-layer capacitor significantly reduced the output voltage loss by providing the necessary power peaks to the system. Our results are consistent with the view that, for the proper operation of the biobattery containing integrated system, the equivalent series resistance of supercapacitor should be on the level of a few hundred of $\text{m}\Omega$ and the leakage current should not exceed a few μA . Furthermore, the capacitance has to be carefully selected to provide the required energy balance. Such optimized system has been found to be potentially suitable to power a digital watch under operating modes having different power demands. Our present results have preliminary character, but they seem to define directions for research aiming at the development of more practical enzyme-based biobatteries and biofuel cells.

Acknowledgments This work was supported by the Polish Ministry of Science and Higher Education and the National Center for Research and Development (NCBiR) under the project NR05-0017-10/2010 (PBR-11).

Open Access This article is distributed under the terms of the Creative Commons Attribution License which permits any use, distribution, and reproduction in any medium, provided the original author(s) and the source are credited.

References

- Tarasevich MR, Yaropolov AI, Bogdanovskaya VA, Varfolomeev SD (1979) Electrocatalysis of a cathodic oxygen reduction by laccase. *Bioelectrochem Bioenergy* 6:393–403
- Eys JV, Kaplan NO (1957) Yeast alcohol dehydrogenase. III. Relation of alcohol structure to activity. *J Am Chem Soc* 79:2782–2786
- Heller A (2004) Miniature biofuel cells. *Chem Phys* 6:209–216
- Persson B, Gorton L, Johansson G, Torstensson A (1985) Biofuel anode based on D-glucose dehydrogenase, nicotinamide adenine dinucleotide and a modified electrode. *Enzyme Microb Technol* 7:549–552
- Willner I, Arad G, Katz E (1998) A biofuel cell based on pyroloquinolinequinone and microperoxidase-11 monolayer-functionalized electrodes. *Bioelectrochem Bioenergy* 44:209–214
- Minteer SD, Liaw BY, Cooney MJ (2007) Enzyme-based biofuel cells. *Curr Opin Biotechnol* 18:228–234
- Barton SC, Gallaway J, Atanassov P (2004) Enzymatic biofuel cells for implantable and microscale devices. *Chem Rev* 104:4867–4886
- Jensen UB, Lorcher S, Vagin M, Chevallerier J, Shipovskov S, Koroleva O, Besenbacher F, Ferapontova EE (2012) A 1.76 V hybrid Zn–O₂ biofuel cell with a fungal laccase-carbon cloth biocathode. *Electrochim Acta* 62:218–226
- Stolarczyk K, Lyp D, Zelechowska K, Biernat JF, Rogalski J, Bilewicz R (2012) Arylated carbon nanotubes for biobatteries and biofuel cells. *Electrochim Acta* 79:74–81
- Nazaruk E, Karaskiewicz M, Zelechowska K, Biernat JF, Rogalski J, Bilewicz R (2012) Powerful connection of laccase and carbon nanotubes: Material for mediator-free electron transport on the enzymatic cathode of the biobattery. *Electrochem Commun* 14:67–70
- Stolarczyk K, Sepelowska M, Lyp D, Zelechowska K, Biernat JF, Rogalski J, Farmer KD, Roberts KN, Bilewicz R (2012) Hybrid biobattery based on arylated carbon nanotubes and laccase. *Bioelectrochem* 87:154–163
- Karaskiewicz M, Nazaruk E, Zelechowska K, Biernat J, Rogalski J, Bilewicz R (2012) Fully enzymatic mediatorless fuel cell with efficient naphthylated carbon nanotube-laccase composite cathodes. *Electrochem Commun* 20:124–127
- Zloczewska A, Jonsson-Niedziolka M (2013) Efficient air-breathing biocathodes for zinc/oxygen batteries. *J Power Sources* 228:104–111
- Ferapontova EE (2006) In: Grimes CA, Dickey EC, Pishko MV (eds) *Encyclopedia of sensors*. American Scientific Publishers, Stevenson Ranch, p 391
- Karnicka K, Miecznikowski K, Kowalewska B, Skunik M, Opallo M, Rogalski J, Schuhmann W, Kulesza PJ (2008) ABTS-modified multiwalled carbon nanotubes as an effective mediating system for bioelectrocatalytic reduction of oxygen. *Anal Chem* 80:7643–7648
- Cardoso FP, Neto SA, Fenga PG, Ciancaglini P, de Andrade AR (2013) Electrochemical characterization of methanol/O₂ biofuel cell: Use of laccase biocathode immobilized with polypyrrole film and PAMAM dendrimers. *Electrochim Acta* 90:90–94
- Ding S-N, Holzinger M, Mousty C, Cosnier S (2010) Laccase electrodes based on the combination of single-walled carbon nanotubes and redox layered double hydroxides: Towards the development of biocathode for biofuel cells. *J Power Sources* 195:4714–4717
- Jenkins P, Tuurala S, Vaari A, Valkiainen M, Smolander M, Leech D (2012) A mediated glucose/oxygen enzymatic fuel cell based on printed carbon inks containing aldose dehydrogenase and laccase as anode and cathode. *Enzyme Microb Technol* 50:181–187
- Barriere F, Ferry Y, Rochefort D, Leech D (2004) Targetting redox polymers as mediators for laccase oxygen reduction in a membrane-less biofuel cell. *Electrochem Commun* 6:237–241
- Swietlikowska A, Gniadek M, Palys B (2013) Electrodeposited grapheme nano-stacks for biosensor applications. Surface groups as redox mediators for laccase. *Electrochim Acta* 98:75–81
- Wang X, Latonen R-M, Sjöberg-Eerola P, Eriksson J-E, Bobacka J, Boer H, Bergelin M (2011) Direct electron transfer of trameteshirsutalaccase in a dual-layer architecture of poly(3,4-ethylenedioxythiophene) films. *J Phys Chem C* 115:5919–5929
- Hussein L, Rubenwolf S, Stetten FV, Urban G, Zengerle R, Krueger M, Kerzenmacher S (2011) A highly efficient buckypaper-based electrode material for mediatorless laccase-catalyzed dioxygen reduction. *Biosens Bioelectron* 26:4133–4138
- Vaz-Dominguez C, Campuzano S, Rudiger O, Pita M, Gorbacheva M, Shleev S, Fernandez VM, De Lacey AL (2008) Laccase electrode for direct electrocatalytic reduction of O₂ to H₂O with high-operational stability and resistance to chloride inhibition. *Biosens Bioelectron* 24:531–537
- Ardhaoui M, Zheng M, Pulpytel J, Dowling D, Jolivald C, Khonsar FA (2013) Plasma functionalized carbon electrode for laccase-catalyzed oxygen reduction by direct electron transfer. *Bioelectrochem* 91:52–61
- Smolander M, Boer H, Valkiainen M, Roozeman R, Bergelin M, Eriksson J-E, Zhang X-C, Koivula A, Viikari L (2008) Development of a printable laccase-based biocathode for fuel cell applications. *Enzyme Microb Technol* 43:93–102
- Choi SH, Kim J, Yoon YS (2004) Fabrication and characterization of a LiCoO₂ battery–supercapacitor combination for a high-pulse power system. *J Power Sources* 138:360–363
- Cericola D, Ruch PW, Kotz R, Novak P, Wokaun A (2010) Simulation of a supercapacitor/Li-ion battery hybrid for pulsed applications. *J Power Sources* 195:2731–2736
- Shin D, Kim Y, Wang Y, Chang N, Pedram M (2012) Constant-current regulator-based battery-supercapacitor hybrid architecture for high-rate pulsed load applications. *J Power Sources* 205:516–524
- Decaux C, Lota G, Raymundo-Pinero E, Frackowiak E, Beguin F (2012) Electrochemical performance of a hybrid lithium-ion capacitor with a graphite anode preloaded from lithium bis(trifluoromethane)sulfonimide-based electrolyte. *Electrochim Acta* 86:282–286
- Ghenaatian HR, Mousavi MF, Rahmanifar MS (2011) High performance battery–supercapacitor hybrid energy storage system based on self-doped polyaniline nanofibers. *Synth Met* 161:2017–2023
- Park K-W, Ahn H-J, Sung Y-E (2002) All-solid-state supercapacitor using Nafion[®] polymer membrane and its hybridization with a direct methanol fuel cell. *J Power Sources* 109:500–506
- Jarvis LP, Atwater TB, Cygan PJ (1999) Fuel cell/electrochemical capacitor hybrid for intermittent high power applications. *J Power Sources* 79:60–63
- Payman A, Pierfederici S, Meibody-Tabar F (2008) Energy control of supercapacitor/fuel cell hybrid power source. *Energy Convers Manage* 49:1637–1644
- Yu Z, Zinger D, Bose A (2011) An innovative optimal power allocation strategy for fuel cell, battery and supercapacitor hybrid electric vehicle. *J Power Sources* 196:2351–2359
- Rodatz P, Paganelli G, Sciarretta A, Guzzella L (2005) Optimal power management of an experimental fuel cell/supercapacitor-powered hybrid vehicle. *Control Eng Pract* 13:41–53
- Keskinen J, Sivonen E, Bergelin M, Eriksson J-E, Sjöberg-Eerola P, Valkiainen M, Smolander M, Vaari A, Uotila J, Boer H,

- Tuurala S (2010) Printed supercapacitor as hybrid device with an enzymatic power source. *Adv Sci Technol* 72:331–336
37. Conway BE (1999) *Electrochemical supercapacitors: scientific fundamentals and technological applications*. Springer, Berlin, pp 1–8
 38. Frackowiak E, Beguin F (2002) Electrochemical storage of energy in carbon nanotubes and nanostructured carbons. *Carbon* 40:1775–1787
 39. Trasatti S, Kurzweil I (1994) Electrochemical supercapacitors as versatile energy stores. *Platinum Metals Rev* 38:46–56
 40. Simon P, Gogotsi Y (2008) Materials for electrochemical capacitors. *Nat Mat* 7:845–854
 41. Lufano F, Staiti P (2004) Performance improvement of Nafion based solid state electrochemical supercapacitor. *Electrochim Acta* 49:2683–2689
 42. Arbizzani C, Biso M, Cericola D, Lazzari M, Soavi F, Mastragostino M (2008) Safe, high-energy supercapacitors based on solvent-free ionic liquid electrolytes. *J Power Sources* 185:1575–1579
 43. Bichat MP, Raymundo-Pinero E, Beguin F (2010) High voltage supercapacitor built with seaweed carbons in neutral aqueous electrolyte. *Carbon* 48:4351–4361
 44. Ruch PW, Kotz R, Wokaun A (2009) Electrochemical characterization of single-walled carbon nanotubes for electrochemical double layer capacitors using non-aqueous electrolyte. *Electrochim Acta* 54:4451–4458
 45. Skunik M, Chojak M, Rutkowska IA, Kulesza PJ (2008) Improved capacitance characteristics during electrochemical charging of carbon nanotubes modified with polyoxometallate monolayers. *Electrochim Acta* 53:3862–3869
 46. Gomez-Romero P, Chojak M, Cuentas-Gallegos K, Asensio JA, Kulesza PJ, Casan-Pastor N, Lira-Cantu M (2003) Hybrid organic-inorganic nanocomposite materials for application in solid state electrochemical supercapacitors. *Electrochem Commun* 5:149–153
 47. Khomenko V, Frackowiak E, Beguin F (2005) Determination of the specific capacitance of conducting polymer/nanotubes composite electrodes using different cell configurations. *Electrochim Acta* 50:2499–2506
 48. Zheng JP, Cygan PJ, Jow TR (1995) Hydrous ruthenium oxide as an electrode material for electrochemical capacitors. *J Electrochem Soc* 142:2699–2703
 49. Rola B, Karaskiewicz M, Majdecka D, Mazur I, Bilewicz R, Ohga S, Rogalski J (2013) Scale up of Cerrena unicolor laccase production. *J Agric Fac Kyushu Univ* 58(2):231–238
 50. Zelechowska K, Stolarczyk K, Lyp D, Rogalski J, Roberts KP, Bilewicz R, Biernat JF (2013) Aryl and *N*-arylamide carbon nanotubes for electrical coupling of laccase to electrodes in biofuel cells and biobatteries. *Biocyber Biomed Eng* 33(4):235–245
 51. Shin W, Lee J, Kim Y, Steinfink H, Heller A (2005) Ionic conduction in $Zn_3(PO_4)_2 \cdot 4H_2O$ enables efficient discharge of the zinc anode in serum. *J Am Chem Soc* 127:14590–14591
 52. Liang P, Huang X, Fan M-Z, Cao X-X, Wang C (2007) Composition and distribution of internal resistance in three types of microbial fuel cells. *Appl Microbiol Biotechnol* 77:551–558
 53. Aiping Y, Chabot V, Zhang J (2013) *Supercapacitors for energy storage and delivery, fundamentals and applications*. CRC Press, Boca Raton